

This article was downloaded by:

On: 28 January 2011

Access details: *Access Details: Free Access*

Publisher *Taylor & Francis*

Informa Ltd Registered in England and Wales Registered Number: 1072954 Registered office: Mortimer House, 37-41 Mortimer Street, London W1T 3JH, UK



Physics and Chemistry of Liquids

Publication details, including instructions for authors and subscription information:

<http://www.informaworld.com/smpp/title~content=t713646857>

Thermodynamics of oxygenate fuel additives as a function of temperature

R. Gonzalez-Olmos^a; M. Iglesias^a; B. M. R. P. Santos^b; S. Mattedi^b

^a Departament d'Enginyeria Química, Escola Tècnica Superior d'Enginyeria Química, Universitat Rovira i Virgili, Tarragona, Espanya ^b Departamento de Engenharia Química, Escola Politécnica, Universidade Federal da Bahia, Brasil

To cite this Article Gonzalez-Olmos, R. , Iglesias, M. , Santos, B. M. R. P. and Mattedi, S.(2008) 'Thermodynamics of oxygenate fuel additives as a function of temperature', *Physics and Chemistry of Liquids*, 46: 3, 223 — 237

To link to this Article: DOI: 10.1080/00319100701660411

URL: <http://dx.doi.org/10.1080/00319100701660411>

PLEASE SCROLL DOWN FOR ARTICLE

Full terms and conditions of use: <http://www.informaworld.com/terms-and-conditions-of-access.pdf>

This article may be used for research, teaching and private study purposes. Any substantial or systematic reproduction, re-distribution, re-selling, loan or sub-licensing, systematic supply or distribution in any form to anyone is expressly forbidden.

The publisher does not give any warranty express or implied or make any representation that the contents will be complete or accurate or up to date. The accuracy of any instructions, formulae and drug doses should be independently verified with primary sources. The publisher shall not be liable for any loss, actions, claims, proceedings, demand or costs or damages whatsoever or howsoever caused arising directly or indirectly in connection with or arising out of the use of this material.

Thermodynamics of oxygenate fuel additives as a function of temperature

R. GONZALEZ-OLMOS*†, M. IGLESIAS†,
B. M. R. P. SANTOS‡ and S. MATTEDI‡

†Departament d'Enginyeria Química, Escola Tècnica Superior d'Enginyeria
Química, Universitat Rovira i Virgili, Avinguda Països Catalans 26,
Campus Sescelades, 43007, Tarragona, Espanya

‡Departamento de Engenharia Química, Escola Politécnica, Universidade
Federal da Bahia, 40210 Salvador-Bahia, Brasil

(Received 22 August 2007; in final form 3 September 2007)

This article reports experimental data of density and ultrasonic velocity at the range from 278.15 to 323.15 K and atmospheric pressure of ethers used as additives in fuels (methyl tert-butyl ether ethyl tert-butyl ether, tert-amyl ether and diisopropyl ether). From the experimental data, temperature dependent polynomials were fitted and theoretical models were used to correlate these properties. The MTC Lattice Gas EOS is used to correlate simultaneously vapour pressures and volumetric properties. Free Length Theory is applied to estimate the ultrasonic velocity of the chemicals as a function of temperature, satisfactory predictions were obtained. The dependence of temperature showed by these magnitudes reveals a strong interaction at low values.

Keywords: Ether; Theoretical model; Density; Ultrasonic velocity; Prediction; Temperature

1. Introduction

Environmental chemistry and engineering need reliable thermodynamic data of pollutants for transfer modelling of organic chemicals, solve the remediation of contaminated soils and waters, minimise the presence of hazardous pollutants in aqueous effluents and develop new strategies for cheap and effective cleaning procedures and then adequate decisions and remediation policies. From a more fundamental point of view, thermodynamics are necessary for the understanding of the complex molecular interactions and mechanisms of the solution. The test of the existent models and the development of new methods for prediction of these thermodynamic functions, have a particular significance because they are the only way to ensure accurate results.

*Corresponding author. Tel.: +34-977-558553. Fax: +34-977-559667. Email: rafael.gonzalez@urv.net

Oxygenated compounds are added to gasoline in order to improve fuel combustion efficiency and to lower exhaust emissions of CO and hydrocarbons. Examples of these compounds are alcohols (as methanol, ethanol, isopropyl alcohol, isobutyl alcohol and tert-butyl alcohol) and ethers (as methyl tert-butyl ether (MTBE), ethyl tert-butyl ether (ETBE), tert-amyl methyl ether (TAME) and diisopropyl ether (DIPE)) [1]. MTBE is the most important fuel oxygenate used worldwide, and from 1998 in USA and 2002 in European Union it was included in monitoring programs of volatile organic compounds and it is considered an unique contaminant due to its ability to move readily throughout various environmental compartments and to its resistance to degradation in all of them except air. On the other hand, MTBE remains in groundwater for a long time after a spill and the other ethers should have similar behaviour due to its similar molecular structure. The contamination of water supplied by these kinds of organic chemicals is a problem of increasing concern in the last few years. Some properties for these compounds are found in literature as Henry's law constants [2], vapour pressures [3]. Vapour pressure is also published as vapour-liquid equilibria data for binary and/or ternary mixtures containing ethers [4-6].

However, systematic studies in terms of wide range of temperature or and pressure of density and ultrasonic velocity are not currently found in the literature. Besides its own practical importance [7], the density and ultrasonic velocity are closely related with the determination of Henry's law constants and the air-water partition coefficients, mass transfer coefficient measurement and calorimetric studies by Maxwell coefficients.

This study is a part of a wider study related to theoretical and experimental analysis of environmental pollutants [8,9]. Thus, as a continuation of our scientific study of investigating physical properties related to characterisation of pollutants, are reported the temperature dependence of density and ultrasonic velocity at the range 278.15-323.15°K and atmospheric pressure of those ethers used in fuels as oxygenated additives. From the experimental data, temperature dependent polynomials were fitted, the corresponding parameters being gathered. Different derived magnitudes from the experimental measurements were calculated. Because of the expense of the experimental measurement of such data and current processes design is strongly computer oriented, consideration was also given attention to how accurate theoretical methods work by comparison with the experimental data. A lattice type equation of state was applied to simultaneously correlate vapour pressure and densities in order to predict the non-ideal temperature dependence of these magnitudes at a wide range. The EOS is based on the generalised van der Waals theory and combines the Staverman-Guggenheim combinatorial term of lattice statistics with an attractive lattice gas expression [10]. They also applied the Free Length Theory (FLT) model to estimate the isentropic compressibility and thus the ultrasonic velocity of the chemicals as a function of temperature as suggested by Jacobsen [11]. Satisfactory predictions were obtained for both properties, a good accuracy being obtained for a wide range of temperatures.

2. Experimental section

2.1. Materials

MTBE, TAME and DIPE were of Merck quality with richness better than 99.5 mol%. ETBE that is provided by REPSOL-YPF has purity higher than 97 mol%. The pure

Table 1. Literature review of physical properties of pure compounds: densities ρ , ultrasonic velocity u .

Component	$T(K)$	$\rho/g\text{ cm}^{-3}$					$u/m\text{ s}^{-1}$			
		exptl.	[12]	[13]	[14]	[15]	exptl.	[15]	[14]	[16]
MTBE	278.15	0.755640	0.75614	–	–	–	–	–	–	–
	280.90	0.752990	–	0.75332	–	–	–	–	–	–
	283.15	0.750684	0.75102	–	–	–	–	–	–	–
	285.90	0.747849	–	0.74811	–	–	–	–	–	–
	288.15	0.745522	0.74585	–	0.7457	0.74579	1082.54	1082.4	1083	–
	288.70	0.745013	–	0.74530	–	–	–	–	–	–
	293.15	0.740336	0.74065	–	0.7404	0.7406	1059.43	1059.5	1060	–
	298.15	0.734915	0.73540	–	0.7353	0.73535	1035.89	1036.1	1035	–
	299.80	0.733068	–	0.73379	–	–	–	–	–	–
	303.15	0.729734	0.73010	–	–	0.73006	1013.37	1013	–	1014
	308.15	0.724277	0.72482	–	–	0.72473	989.91	990.1	–	–
	313.15	0.718875	0.71942	–	–	–	–	–	–	–
		exptl.	[13]	[17]	[18]	exptl.				
	ETBE	280.90	0.752970	0.75316	–	–	–	–	–	–
283.20		0.750709	0.75077	–	–	–	–	–	–	–
285.90		0.747922	0.74799	–	–	–	–	–	–	–
288.70		0.745106	0.74511	–	–	–	–	–	–	–
293.15		0.740503	–	0.74111	–	–	–	–	–	–
298.15		0.735357	–	0.73559	0.7362	1033.23	Not available	–	–	–
299.80		0.733544	0.73373	–	–	–	–	–	–	–
303.15		0.730171	–	0.73085	–	–	–	–	–	–
308.15		0.724947	–	0.72598	–	–	–	–	–	–
313.15		0.719680	–	0.72069	–	–	–	–	–	–
	exptl.	[19]	[18]	exptl.	[18]					
TAME	298.15	0.765399	0.76577	0.7658	1115.55	1115	–	–	–	–
		exptl.	[20]	[21]	[22]	exptl.	[23]	–	–	–
DIPE	288.15	0.728594	–	0.72909	–	–	–	–	–	–
	298.15	0.718207	0.71814	0.71870	0.71840	–	–	–	–	–
	303.15	0.712956	–	–	–	976.04	974.9	–	–	–
	308.15	0.707664	–	0.70812	–	–	–	–	–	–

compounds were stored protected from the sunlight at constant humidity and temperature. All products were degassed using ultrasound and dried on molecular sieves (pore diameter of 4 and 5×10^{-10} m from Fluka) before use. Densities and ultrasonic velocities of the pure substances were checked and listed in table 1 and compared with literature values.

2.2. Apparatus and procedure

The ultrasonic velocities and densities were measured with an Anton Paar DSA-5000 device with a precision of $\pm 0.1\text{ m s}^{-1}$ and $\pm 10^{-6}\text{ g cm}^{-3}$. The temperature was kept constant with an accuracy of 0.001 K. Calibration of the apparatus was performed periodically, in accordance with technical specifications, using Millipore quality water (resistivity, 18.2 M Ω cm) and ambient air. Experimental procedure in our laboratory is explained in detail in earlier papers.

3. Results and discussion

3.1. Data correlation

The experimental measurements are presented in table 2. For compact and smooth representation, the density and ultrasonic velocity of the chemicals were correlated as a function of temperature in accordance to the equation 1:

$$z = \sum_{i=0}^N A_i T^i. \quad (1)$$

Where z is density (gcm^3) or ultrasonic velocity (ms^{-1}), T is the absolute temperature in Kelvin and A_i are fitting parameters. N stands for the extension of the mathematical series, which was optimised by means of the Bevington test [24]. The fitting parameters were obtained by the unweighted least squared method applying a fitting Marquardt algorithm. The root mean square deviations were computed using equation 2, where z is the value of the property, and n_{DAT} is the number of experimental data.

$$\sigma = \left(\frac{\sum_{i=1}^{n_{\text{DAT}}} (z_{\text{exp}} - z_{\text{pred}})^2}{n_{\text{DAT}}} \right)^{1/2}. \quad (2)$$

The fitting parameters and the corresponding deviations are gathered in table 3. Figures 1 and 2, show the trend of density and ultrasonic velocity as a temperature function.

3.2. Derived properties

A frequently applied derived magnitude for chemicals is the temperature dependence of volumetry, which is expressed as isobaric expansibility or thermal expansion coefficient (α). The data reported in literature normally give only values of thermal expansion coefficients both of pure compounds and its mixtures, showing the relative changes in density, calculated by means of $-(\Delta\rho/\rho)$ as a function of temperature and assuming that α remains constant in any thermal range. This fact is due to the scarce availability of accurate density data in a wide temperature range. The pure chemicals can be computed by the following expression:

$$\alpha = - \left(\frac{\partial \ln \rho}{\partial T} \right)_p. \quad (3)$$

The values of isobaric expansibility computed from the measured densities are gathered in table 2. The trend of isobaric expansibility is enclosed in figure 3(a)).

It has been attempted to explain the physico-chemical behaviour of the compounds indicated above, in order to explore the strength and nature of the interactions of the components by deriving various thermodynamic parameters from the ultrasonic velocity and density data. The parameters derived from the experimental measured data

Table 2. Densities, ultrasonic sound and derived properties of the used chemicals at the range of temperature 278.15–323.15 K.

$T(K)$ MTBE	ρ/gcm^{-3}	u/ms^{-1}	κ_S/TPa^{-1}	$10^3 \alpha/K^{-1}$	S	$Z/gcm^{-3}ms^{-1}$	$T(K)$	ρ/gcm^{-3}	u/ms^{-1}	κ_S/TPa^{-1}	$10^3 \alpha/K^{-1}$	S	$Z(gcm^{-3}ms^{-1})$
323.150	0.707917	922.21	1660.956	1.570	2.504	652.848	300.154	0.732911	1027.40	1292.616	1.448	2.766	752.993
322.152	0.709013	926.54	1642.924	1.564	2.515	656.929	299.151	0.733858	1031.27	1281.277	1.443	2.776	756.806
321.155	0.710119	930.98	1624.756	1.558	2.526	661.107	298.151	0.734915	1035.89	1268.048	1.439	2.787	761.291
320.156	0.711220	935.49	1606.637	1.552	2.537	665.339	297.150	0.735969	1040.52	1254.988	1.434	2.799	765.790
319.156	0.712322	939.99	1588.829	1.546	2.548	669.576	296.156	0.737188	1045.49	1241.029	1.430	2.811	770.723
318.155	0.713419	944.49	1571.305	1.540	2.560	673.817	295.149	0.738067	1049.80	1229.394	1.426	2.822	774.823
317.155	0.714516	949.00	1554.016	1.534	2.571	678.076	294.150	0.739115	1054.44	1216.870	1.421	2.833	779.352
316.155	0.715610	953.51	1536.997	1.529	2.582	682.341	293.150	0.740336	1059.43	1203.446	1.417	2.846	784.334
315.156	0.716702	958.00	1520.304	1.523	2.593	686.601	292.150	0.741203	1063.72	1192.362	1.413	2.856	788.432
314.155	0.717789	962.52	1503.778	1.518	2.605	690.886	291.148	0.742245	1068.35	1180.390	1.409	2.868	792.977
313.155	0.718875	967.07	1487.410	1.512	2.616	695.202	290.148	0.743285	1073.05	1168.435	1.405	2.879	797.582
312.153	0.719963	971.64	1471.225	1.507	2.627	699.545	289.148	0.744324	1077.77	1156.607	1.402	2.891	802.210
311.155	0.721043	976.21	1455.299	1.502	2.639	703.889	288.147	0.745522	1082.54	1144.594	1.398	2.903	807.057
310.156	0.722122	980.77	1439.644	1.496	2.650	708.236	287.147	0.746397	1087.21	1133.452	1.394	2.915	811.490
309.153	0.723202	985.34	1424.191	1.491	2.661	712.600	286.145	0.747592	1092.65	1120.400	1.390	2.928	816.856
308.156	0.724277	989.91	1408.977	1.486	2.673	716.969	285.145	0.748623	1097.33	1109.334	1.387	2.940	821.486
307.155	0.725349	994.48	1393.994	1.481	2.684	721.345	284.144	0.749654	1102.04	1098.359	1.383	2.951	826.149
306.155	0.726540	999.41	1378.012	1.476	2.697	726.111	283.144	0.750684	1106.78	1087.477	1.380	2.963	830.842
305.155	0.727489	1003.64	1364.639	1.471	2.707	730.137	282.146	0.751711	1111.51	1076.769	1.376	2.975	835.534
304.155	0.728671	1008.71	1348.764	1.466	2.720	735.018	281.147	0.752735	1116.21	1066.267	1.373	2.986	840.210
303.154	0.729734	1013.37	1334.441	1.462	2.731	739.491	280.145	0.753760	1120.89	1055.944	1.370	2.998	844.882
302.154	0.730795	1018.04	1320.306	1.457	2.743	743.979	279.144	0.754783	1125.62	1045.669	1.366	3.010	849.599
301.154	0.731853	1022.72	1306.359	1.452	2.755	748.481	278.142	0.755640	1130.08	1036.255	1.363	3.021	853.934
ETBE													
323.150	0.709007	922.48	1657.431	1.519	2.494	654.045	315.155	0.717560	957.23	1520.930	1.480	2.580	686.870
322.153	0.710068	926.65	1640.093	1.514	2.504	657.985	314.155	0.718620	961.65	1504.758	1.475	2.591	691.061
321.156	0.711143	930.99	1622.382	1.509	2.515	662.067	313.154	0.719680	966.09	1488.762	1.470	2.602	695.276
320.154	0.712240	935.26	1605.125	1.504	2.526	666.130	312.154	0.720737	970.55	1472.948	1.466	2.614	699.511
319.155	0.713302	939.61	1587.930	1.499	2.536	670.226	311.154	0.721793	975.01	1457.368	1.461	2.625	703.755
318.156	0.714370	944.02	1570.777	1.494	2.547	674.380	310.154	0.722845	979.47	1442.024	1.456	2.636	708.005
317.154	0.715436	948.42	1553.917	1.489	2.558	678.534	309.154	0.723897	983.92	1426.933	1.452	2.647	712.257
316.155	0.716498	952.82	1537.316	1.484	2.569	682.694	308.154	0.724947	988.39	1412.008	1.448	2.658	716.530
307.154	0.725995	992.85	1397.330	1.443	2.669	720.804	292.150	0.741529	1060.43	1199.245	1.381	2.837	786.340
306.154	0.727042	997.30	1382.894	1.439	2.680	725.079	291.149	0.742552	1064.95	1187.448	1.377	2.848	790.781
305.154	0.728086	1001.77	1368.615	1.434	2.691	729.375	290.148	0.743573	1069.52	1175.706	1.373	2.859	795.266

(Continued)

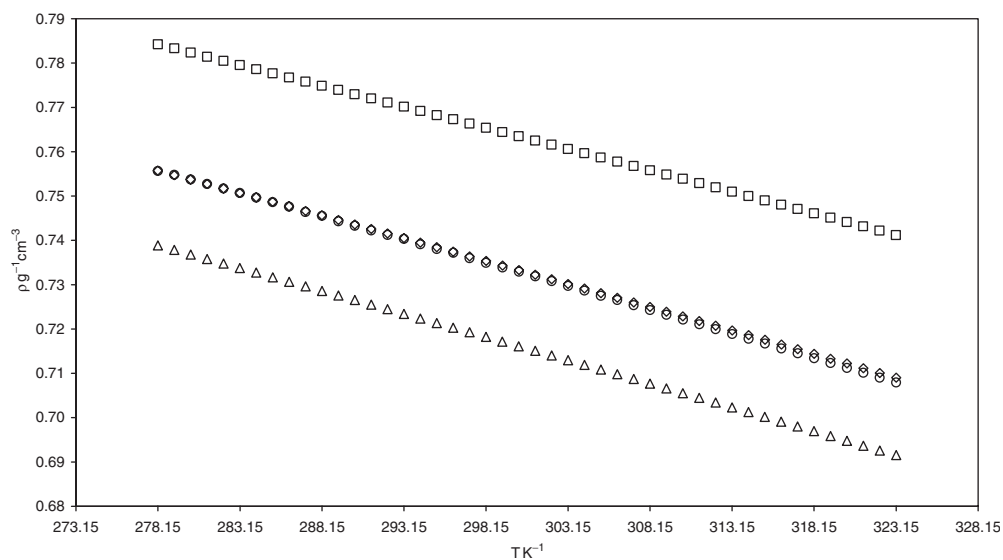
Table 2. Continued.

$T(K)$	ρ/gcm^{-3}	u/ms^{-1}	κ_s/TPa^{-1}	$10^3 \alpha/\text{K}^{-1}$	S	$Z/\text{gcm}^{-3}\text{ms}^{-1}$	$T(K)$	ρ/gcm^{-3}	u/ms^{-1}	κ_s/TPa^{-1}	$10^3 \alpha/\text{K}^{-1}$	S	$Z(\text{gcm}^{-3}\text{ms}^{-1})$
304.153	0.729127	1006.24	1354.546	1.430	2.702	733.677	289.149	0.744596	1074.12	1164.056	1.369	2.871	799.785
303.153	0.730171	1010.71	1340.671	1.426	2.713	737.991	288.146	0.745656	1078.87	1152.188	1.366	2.882	804.466
302.153	0.731209	1015.19	1326.978	1.421	2.724	742.316	287.151	0.746644	1083.04	1141.819	1.362	2.893	808.645
301.152	0.732248	1019.69	1313.426	1.417	2.736	746.666	286.145	0.747668	1087.69	1130.527	1.358	2.904	813.231
300.151	0.733283	1024.20	1300.046	1.413	2.747	751.028	285.144	0.748683	1092.33	1119.423	1.355	2.916	817.809
299.152	0.734319	1028.71	1286.854	1.409	2.758	755.401	284.142	0.749696	1096.95	1108.514	1.351	2.927	822.379
298.152	0.735357	1033.23	1273.819	1.405	2.769	759.793	283.141	0.750709	1101.58	1097.732	1.348	2.938	826.966
297.151	0.736390	1037.76	1260.951	1.401	2.780	764.196	282.142	0.751709	1106.20	1087.134	1.344	2.950	831.540
296.150	0.737420	1042.28	1248.292	1.397	2.792	768.598	281.141	0.752719	1110.84	1076.624	1.341	2.961	836.150
295.150	0.738448	1046.81	1235.789	1.393	2.803	773.015	280.139	0.753739	1115.50	1066.203	1.337	2.973	840.796
294.150	0.739476	1051.36	1223.413	1.389	2.814	777.455	279.141	0.754735	1120.14	1055.993	1.334	2.984	845.409
293.149	0.740503	1055.90	1211.233	1.385	2.825	781.897	278.140	0.755742	1124.79	1045.884	1.330	2.996	850.051
TAME													
323.147	0.741199	1008.07	1327.651	1.330	2.711	747.180	303.146	0.760625	1093.74	1099.009	1.259	2.924	831.926
322.146	0.742182	1012.27	1314.912	1.326	2.722	751.289	302.146	0.761581	1098.10	1088.930	1.256	2.935	836.292
321.147	0.743166	1016.51	1302.239	1.322	2.732	755.436	301.147	0.762538	1102.46	1078.979	1.253	2.945	840.668
320.146	0.744148	1020.77	1289.689	1.319	2.743	759.604	300.146	0.763493	1106.82	1069.156	1.250	2.956	845.049
319.146	0.745128	1025.00	1277.384	1.315	2.753	763.756	299.146	0.764446	1111.17	1059.479	1.247	2.967	849.429
318.146	0.746106	1029.25	1265.196	1.311	2.764	767.930	298.147	0.765399	1115.55	1049.866	1.244	2.978	853.841
317.148	0.747084	1033.52	1253.120	1.307	2.775	772.126	297.146	0.766350	1119.93	1040.378	1.241	2.989	858.258
316.146	0.748060	1037.77	1241.256	1.304	2.785	776.314	296.147	0.767302	1124.28	1031.062	1.238	2.999	862.662
315.146	0.749034	1042.05	1229.480	1.300	2.796	780.531	295.145	0.768251	1128.69	1021.757	1.235	3.010	867.117
314.146	0.750009	1046.32	1217.880	1.297	2.806	784.749	294.146	0.769199	1133.13	1012.516	1.232	3.021	871.602
313.146	0.750979	1050.61	1206.394	1.293	2.817	788.986	293.147	0.770147	1137.51	1003.497	1.229	3.032	876.050
312.147	0.751949	1054.88	1195.103	1.290	2.828	793.216	291.146	0.772038	1146.31	985.728	1.224	3.054	884.995
311.147	0.752917	1059.17	1183.918	1.286	2.838	797.467	290.144	0.772983	1150.73	976.974	1.221	3.065	889.495
310.146	0.753887	1063.48	1172.830	1.283	2.849	801.744	289.145	0.773926	1155.15	968.331	1.218	3.076	894.001
309.147	0.754853	1067.77	1161.936	1.279	2.860	806.009	288.146	0.774869	1159.58	959.777	1.216	3.087	898.523
308.146	0.755820	1072.07	1151.159	1.276	2.870	810.292	287.145	0.775810	1164.01	951.330	1.213	3.097	903.051
307.147	0.756783	1076.38	1140.506	1.272	2.881	814.586	286.146	0.776751	1168.44	942.986	1.211	3.108	907.587
306.147	0.757746	1080.71	1129.947	1.269	2.892	818.904	285.146	0.777689	1172.88	934.732	1.208	3.119	912.136
305.146	0.758707	1085.05	1119.506	1.266	2.902	823.235	284.146	0.778629	1177.33	926.559	1.205	3.130	916.703
304.146	0.759666	1089.39	1109.202	1.263	2.913	827.573	283.146	0.779569	1181.78	918.485	1.203	3.141	921.279
282.144	0.780505	1186.20	910.560	1.200	3.152	925.835	279.146	0.783315	1199.56	887.196	1.193	3.185	939.633
281.145	0.781443	1190.65	902.681	1.198	3.163	930.425	278.151	0.784240	1203.85	879.845	1.191	3.196	944.107
280.145	0.782378	1195.12	894.871	1.196	3.174	935.036							

DIPE	323.151	0.691533	888.61	1831.322	1.581	2.407	614.503	297.150	0.719254	1002.68	1382.907	1.452	2.691	721.182
	322.151	0.692581	893.12	1810.130	1.575	2.419	618.558	296.149	0.720295	1007.13	1368.732	1.448	2.703	725.431
	321.151	0.693673	897.45	1789.883	1.570	2.429	622.537	295.150	0.721338	1011.61	1354.675	1.444	2.714	729.713
	320.152	0.694761	901.76	1770.038	1.564	2.440	626.508	294.150	0.722378	1016.11	1340.769	1.440	2.725	734.016
	319.150	0.695848	906.07	1750.500	1.559	2.451	630.487	293.150	0.723416	1020.59	1327.117	1.435	2.736	738.311
	318.149	0.696931	910.40	1731.194	1.554	2.462	634.486	292.150	0.724455	1025.06	1313.681	1.431	2.747	742.610
	317.150	0.698014	914.73	1712.182	1.548	2.473	638.494	291.149	0.725491	1029.54	1300.414	1.427	2.758	746.922
	316.151	0.699093	919.08	1693.396	1.543	2.483	642.522	290.148	0.726528	1034.04	1287.280	1.423	2.769	751.259
	315.150	0.700173	923.44	1674.855	1.538	2.494	646.568	289.149	0.727562	1038.53	1274.359	1.420	2.780	755.595
	314.151	0.701248	927.80	1656.608	1.533	2.505	650.618	288.148	0.728594	1043.03	1261.597	1.416	2.792	759.945
	313.151	0.702321	932.17	1638.604	1.527	2.516	654.683	287.149	0.729624	1047.51	1249.064	1.412	2.803	764.288
	312.150	0.703395	936.55	1620.835	1.522	2.527	658.765	286.148	0.730653	1051.96	1236.774	1.408	2.814	768.618
	311.151	0.704464	940.91	1603.412	1.517	2.538	662.837	285.149	0.731683	1056.44	1224.581	1.404	2.825	772.979
	310.150	0.705531	945.30	1586.151	1.512	2.549	666.938	284.148	0.732709	1060.90	1212.606	1.401	2.836	777.331
	309.150	0.706597	949.67	1569.216	1.507	2.560	671.034	283.149	0.733735	1065.39	1200.725	1.397	2.847	781.714
	308.150	0.707664	954.04	1552.529	1.503	2.571	675.140	282.148	0.734759	1069.91	1188.942	1.394	2.858	786.126
	307.150	0.708726	958.43	1536.034	1.498	2.582	679.264	281.149	0.735783	1074.44	1177.297	1.390	2.869	790.555
	306.150	0.709785	962.82	1519.788	1.493	2.592	683.395	280.900	0.736807	1078.95	1174.484	1.389	2.872	791.637
	305.149	0.710845	967.22	1503.746	1.488	2.603	687.544	280.647	0.736294	1076.68	1171.589	1.388	2.875	792.753
	304.150	0.711900	971.63	1487.919	1.484	2.614	691.703	280.398	0.736549	1077.81	1168.729	1.388	2.878	793.860
	303.150	0.712956	976.04	1472.319	1.479	2.625	695.874	280.148	0.736806	1078.95	1165.854	1.387	2.880	794.977
	302.150	0.714010	980.48	1456.861	1.474	2.636	700.073	279.898	0.737061	1080.08	1163.013	1.386	2.883	796.085
	301.150	0.715063	984.91	1441.659	1.470	2.647	704.273	279.648	0.737316	1081.20	1160.204	1.385	2.886	797.186
	300.149	0.716112	989.35	1426.656	1.465	2.658	708.485	279.398	0.737571	1082.32	1157.404	1.384	2.889	798.288
	299.149	0.717161	993.78	1411.896	1.461	2.669	712.700	279.147	0.737827	1083.45	1154.590	1.383	2.892	799.399
	298.150	0.718207	998.23	1397.298	1.457	2.680	716.936	278.151	0.738843	1087.84	1143.715	1.380	2.902	803.743

Table 3. Parameters of eq 2 in the range 283.15–323.15 K and root mean square deviations (σ).

	A_0	A_1	A_2	A_3	σ
Density/(gcm^{-3})					
MTBE	7.604×10^{-1}	-9.788×10^{-4}	-1.716×10^{-6}	2.000×10^{-9}	4.213×10^{-5}
ETBE	7.608×10^{-1}	-1.001×10^{-3}	-5.007×10^{-7}	-3.469×10^{-9}	6.082×10^{-6}
TAME	7.889×10^{-1}	-9.306×10^{-4}	-3.074×10^{-7}	-3.292×10^{-9}	1.344×10^{-6}
DIPE	7.439×10^{-1}	-1.014×10^{-3}	-4.850×10^{-7}	-4.107×10^{-9}	3.351×10^{-6}
Ultrasonic velocity/(ms^{-1})					
MTBE	1.153×10^3	-4.848	4.884×10^{-3}	-1.903×10^{-5}	1.238×10^{-1}
ETBE	1.148×10^3	-4.649	2.464×10^{-3}	5.395×10^{-6}	6.448×10^{-2}
TAME	1.226×10^3	-4.480	1.473×10^{-3}	1.623×10^{-5}	2.758×10^{-2}
DIPE	1.111×10^3	-4.517	4.634×10^{-4}	2.404×10^{-5}	3.836×10^{-2}

Figure 1. Plots of density (gcm^{-3}) of MTBE (\circ), ETBE (\diamond), TAME (\square) and DIPE (\triangle) at the range of temperatures 278.15–323.15 K.

were isentropic compressibility (k_s), collision factor (S) and specific acoustic impedance (Z), attending to the following set of equations:

$$k_s = \left(\frac{1}{u^2 \cdot \rho} \right) \quad (4)$$

$$Z = u \cdot \rho \quad (5)$$

$$S = \frac{u \cdot V}{B \cdot u_\infty} \quad (6)$$

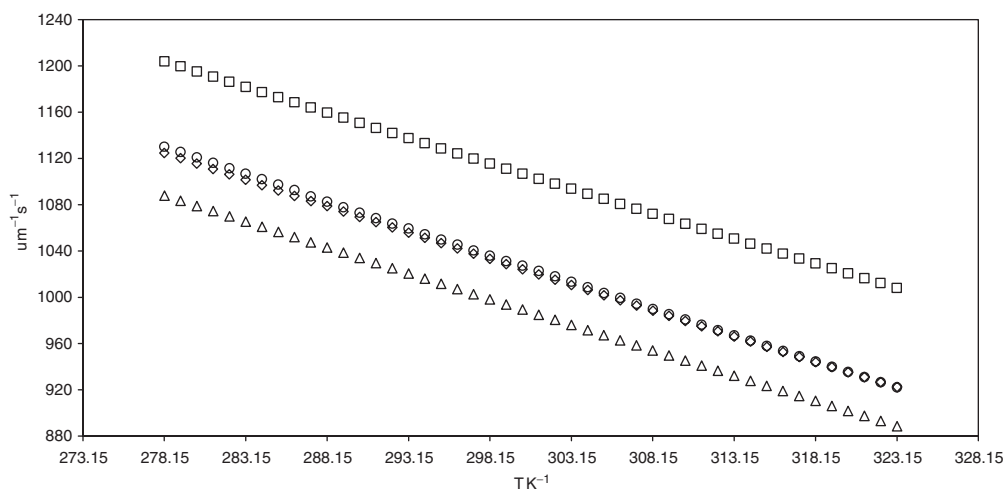


Figure 2. Plots of ultrasonic velocity (ms^{-1}) of MTBE (\circ), ETBE (\diamond), TAME (\square) and DIPE (\triangle) at the range of temperatures 278.15–323.15 K.

Where u_{∞} is taken as 1600 ms^{-1} [11], V is the molar volume and B is the geometrical volume that is defined by the following equation:

$$B = \left(\frac{4}{3}\right)\pi r^3 N. \quad (7)$$

Where N is the Avogadro number and r is the molecular radius calculated through the following expression:

$$r = \left(\frac{3b}{16\pi N}\right)^{1/3}. \quad (8)$$

Where b is the Van der Waals constant and is calculated from density and speed of sounds measurements with the following equation:

$$b = \left(\frac{M}{\rho}\right) - \left(\frac{RT}{\rho \cdot u^2}\right) \cdot \left(\left[1 + \frac{M \cdot u^2}{3RT}\right]^{1/2} - 1\right). \quad (9)$$

Where R and π are common universal constants ($8.3145 \text{ Jmol}^{-1} \text{ K}^{-1}$ and 3.141596 , respectively) and M is the molecular weight. The values of κ_s , S and Z are enclosed into the table 2. In figures 3(b)–(d) the temperature trend of the isentropic compressibility, collision factor and the specific acoustic impedance, respectively, are shown.

It is seen from the measured data that an intense effect of temperature is produced in the compounds. In fact, density and ultrasonic velocity decrease as temperature rises. The molecular association becomes higher, then, at the lowest temperature, where velocity and density have high values. This may be interpreted due to the formation of stable polar interactions among ether group resulting into complex formation producing displacement of electrons and nuclei. The occurrence of high values is for TAME due to its lower steric hindrance of aliphatic ends around oxygen. The observed decrease of velocity with temperature may be explained by an increment in entropy and

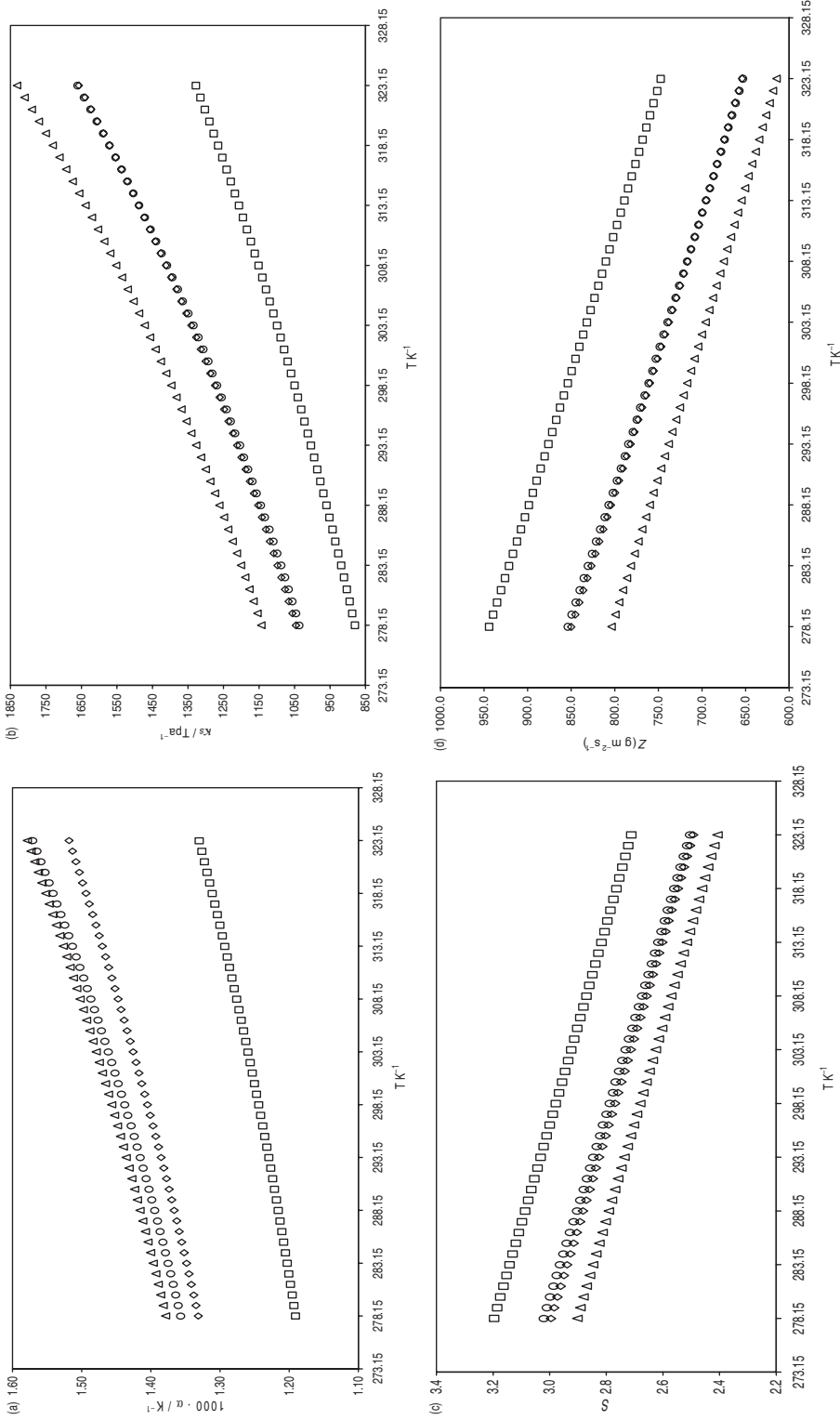


Figure 3. Plots of derived properties (a) isentropic compressibility (TPa^{-1}), (b) isobaric expansivity (α , K^{-1}), (c) collision factor, (d) specific acoustic impedance ($\text{gm}^{-3} \text{ ms}^{-1}$) of MTBE (○), ETBE (◇), TAME (□) and DIPE (△) at the range of temperatures 278.15–323.15 K.

a diminution of ether groups interaction power by steric hindrance. The weakening of the intermolecular forces is probably the reason for strong decrease in ultrasonic velocity at any case. As it could be expected, attending to the molecular structure of solvents, three different trends of interaction could be observed: a strong package capability for TAME molecules, second, a similar trend for MTBE and ETBE and finally a lower density and ultrasonic velocity due to chemical structure of DIPE.

Temperature is a fact that this study deals towards diminution of both measured magnitudes, probably due to an increasing difficult of accommodation of the aliphatic ends of the ethers by molecular kinetics into an ordered structure. Steric hindrance is of course the main factor. In the last few years, different studies have pointed out the special "iceberg structure" of hydroxyl short molecules, specially water, alcohols and aqueous mixtures of alcohols, and the intense modifications that this structure suffers as a function of composition and temperature. This special structure is especially sensitive to the introduction of globular molecules as those studied here, with polar or slight polar groups, as occurs when these compounds are spilled into environment. When these substances are pure compounds, as observed, steric hindrance weakens polar interactions among like molecules when temperature rises, resulting into formation of short mean life polar interactions and then less rigid liquid solvents. Intermolecular free length shows an analogous behaviour as reflected by isentropic compressibility for this mixture (equation 22). The decreased compressibility towards lower temperatures brings the molecules to a closer packing, resulting into a decrease of intermolecular free length. The decrease in the values of isentropic compressibility (figure 3(b)) and intermolecular free length with increase in ultrasonic velocity indicates that there is a significant interaction among molecules due to, which structural arrangement is considerably affected. Figure 3(a) tallies with this idea, showing rising values of isobaric expansibility for increasing temperatures for the whole compounds. Accordingly to this fact, the collision factor diminishes due to a larger distance among molecules (figure 3(c)). About the obtained values for the acoustic impedance for all compounds (figure 3(d)), decrease in an analogous way, they reveal a lower molecular interaction when temperature rises and then a lower acoustic pressure into the liquid media.

3.3. Estimation of density-MTC lattice gas EOS

In the last few years, many researchers have applied and modify cubic equations of state to almost any situation for thermodynamic studies of pure chemicals and mixtures, although the success is always strongly dependent of a wide understanding of how molecules interact in terms of space and energy [25]. However, in the last few years the interest related to non-cubic theoretically based EOS for prediction of fluid phase equilibria or others thermodynamical properties has increased. In this study, the Lattice gas EOS developed by [10] was also used to describe volumetric trend of these chemicals. The EOS is normally written in groups contribution form, which is:

$$z = \tilde{v}r \ln \left[\frac{\tilde{v}}{\tilde{v}-1} \right] + \frac{Z}{2} \tilde{v}r \ln \left[\frac{\tilde{v}-1+(q/r)}{\tilde{v}} \right] + l - \frac{\tilde{v}\Psi(q/r)}{\tilde{v}-1+(q/r)} \sum_{i=1}^{n_c} \sum_{a=1}^{n_g} x_i v_i^a Q^a \frac{(\Gamma^a - 1)}{\tilde{v}-1+(q/r)\Gamma^a}. \quad (10)$$

Where z is the compressibility factor, v_i^a is the number of type a groups in a molecule of type i , Q^a is the surface area of group a , $l = (Z/2)(r - q) - (r - 1)$ and Ψ is a constant of the lattice structure, set to 1. The average number of segments occupied by a molecule in the lattice (r), the mean number of nearest neighbours (Zq) and the reduced molar volume (\tilde{v}) are given by:

$$r_i = \sum_a v_i^a R_a r = \sum_i x_i r_i \quad (11)$$

$$Zq = \sum_{i=1}^{n_c} x_i \sum_{a=1}^{n_g} v_i^a Z Q^a \quad (12)$$

$$\tilde{v} = \frac{V}{N r V^*} = \frac{v}{r v^*} \quad (13)$$

$$r V^* = \sum_{i=1}^{n_c} x_i \sum_{a=1}^{n_g} v_i^a V^a \quad (14)$$

$$r v^* = \sum_{i=1}^{n_c} x_i \sum_{a=1}^{n_g} v_i^a v^a. \quad (15)$$

Here, R^a and V^a are the group-contribution parameters for the number of segments and hard-core volume, respectively; v^a is the molar hard-core volume parameter for a group of type a . There was also defined:

$$\Gamma^a = \sum_{m=1}^{n_g} S^m \gamma^{ma} \quad (16)$$

$$S^m = \frac{\sum_{i=1}^{n_c} v_i^m x_i Q^m}{q} \quad (17)$$

$$\gamma^{ma} = \exp\left(\frac{-u^{ma}}{(RT)}\right). \quad (18)$$

Where u^{ma} is the interaction energy between groups m and a . The fugacity coefficient derived for the model is:

$$\begin{aligned} \ln \hat{\phi}_i = & -r_i \ln \left[\frac{\tilde{v} - 1}{\tilde{v} - 1 + (q/r)} \right] + (1 - l_i) \ln \left[\frac{\tilde{v}}{\tilde{v} - 1 + (q/r)} \right] + \frac{\Psi(q/r)(q_i - r_i)}{\tilde{v} - 1 + (q/r)} \\ & + \Psi \sum_{a=1}^{n_g} v_i^a Q^a \ln \left[\frac{\tilde{v} - 1 + (q/r)}{\tilde{v} - 1 + (q/r) \Gamma^a} \right] - \frac{\Psi}{r} \sum_{k=1}^{n_c} \sum_{a=1}^{n_g} x_k v_k^a Q^a \frac{(\sum_{e=1}^{n_g} v_i^e Q^e \gamma^{ea} - r_i)}{\tilde{v} - 1 + (q/r) \Gamma^a} - \ln z. \quad (19) \end{aligned}$$

It was assumed in previous studies that u^{ba} are given by:

$$\frac{u^{ba}}{R} = \frac{u_0^{ba}}{R} \left(1 + \frac{B^{ba}}{T} \right). \quad (20)$$

In summary, the equation of state has four parameters for each group (v^a , Q^a , u_0^{aa}/R and B^{aa}) and two parameters for interactions between unlike groups (u_0^{ba}/R and B^{ba}).

Table 4. Obtained parameters for EOS root mean square deviation between calculated and experimental values for vapour pressure (P^{sat}) and liquid density (ρ).

Component	v^a $\text{cm}^3 \text{mol}^{-1}$	Q^a	B^{aa} K	u_0^{aa}/R^{-1} K
MTBE	84.235	10.622	16.965	-337.186
ETBE	97.046	12.304	8.9901	-338.429
TAME	95.559	12.045	10.003	-353.999
DIPE	100.79	12.037	39.833	-271.810

The cell volume v^* is fixed in $5 \text{ cm}^3 \text{ mol}^{-1}$ was used as suggested by Mattedi *et al.* Although the EOS is written in a group contribution form, in this study a molecular approach was used, and so each compound were considered as a group. Pure parameters were fitted using the simplex algorithm of Nelder and Mead [26], in order to minimise the objective function:

$$F = \frac{\sum_{i=1}^N \left[\left(\frac{P_{i,\text{cal}}^{\text{sat}} - P_{i,\text{pex}}^{\text{sat}}}{P_{i,\text{pex}}^{\text{sat}}} \right)^2 + \left(\frac{\rho_{i,\text{cal}}^{\text{liq-sat}} - \rho_{i,\text{pex}}^{\text{liq-sat}}}{\rho_{i,\text{pex}}^{\text{liq-sat}}} \right)^2 \right]}{N} \quad (21)$$

Where P^{sat} is the vapour pressure and $\rho^{\text{liq-sat}}$ is the saturated molar liquid density. The subscripts cal and pex indicate calculated and pseudo-experimental values and N is the number of data points used. The numerical values for the obtained parameters are coherent. As expected, similar parameters for all substances have the same magnitude. Vapour pressure experimental data were obtained from [3], except for DIPE, which direct data was not available. For DIPE there were used pseudo-experimental data generated through DIPPR correlation [27] in the range of 5–50°C. Experimental density data from this study was also used. Table 4 presents the obtained parameters. The numerical values for the obtained parameters are coherent. As expected, similar parameters for all substances have the same magnitude. Only the energy parameter and the parameter for its temperature dependency are different for DIPE. It could be explained because pseudo-experimental data of vapour pressure used in fitting procedure was in the range from 5–50°C, the data available for the others ethers were in a wider range of temperature. In table 5, the root mean square deviations and the relative deviation for vapour pressure and liquid density are shown. From the presented results it could be seen that a very good agreement between experimental and calculated values for the two properties.

3.4. Estimation of ultrasonic velocity – FLT

In the last few years, FLT has proved its applicability for multicomponent estimation and accurate results for molecules of different nature. The experimental data for the isentropic compressibility of the chemicals studied here were compared with values determined by the theoretical procedures. This model could be expressed as follows [11]:

$$\kappa_s = \left(\frac{L_f^2}{K^2} \right) \quad (22)$$

Table 5. Comparison obtained between experimental data and theories (root mean square (σ) and relative deviations).

Component	P^{sat}		ρ^{liq}		FLT
	σ	$\Delta P/P$ (%)	σ	$\Delta \rho/\rho$ (%)	σ
MTBE	0.002930	0.06	0.019437	2.66	43.021
ETBE	0.000420	0.07	0.001123	0.13	45.448
TAME	0.000347	0.10	0.000930	0.11	36.102
DIPE	0.000647	0.12	0.001489	0.18	31.857

Where κ_s is the isentropic compressibility that is calculated with the ultrasonic velocity (u) and density (ρ), through the equation 4:

K is a temperature dependent constant ($K = (93.875 + 0.375 \cdot T) \cdot 10^{-8}$) and L_f is the intermolecular free length calculated by the following expression:

$$L_f = \left(\frac{2 \cdot (V - V_0)}{Y} \right). \quad (23)$$

Where V_0 is the molar volume at absolute zero and Y is the molar surface area. These two variable are calculated with the next equations:

$$Y = 408402519.1 \cdot (V_0)^{(2/3)} \quad (24)$$

$$V_0 = V \cdot \left(1 - \frac{T}{T_c} \right)^{0.3}. \quad (25)$$

Where T_c are the critical temperatures and were used the published in literature [28].

The FLT estimates the isentropic compressibility of a mixture attending to the free displacement of molecules as a main function of temperature. The deviations of each procedure for the studied mixtures are gathered into table 5 by means of equation 22, giving the FLT acceptable results in terms of quantity and sign at every studied case.

4. Conclusions

It is well known that thermodynamic properties govern the behaviour of contaminants in the environment. Values of basic magnitudes as density, ultrasonic velocities and isentropic compressibilities can thus be applied to model and predict the displacement, distribution and fate of contaminants into natural media. In this article, new data for the temperature dependence of density and ultrasonic velocity at the range of temperature 278.15–323.15 K and atmospheric pressure of a collection of ethers applied as gasoline oxygenated additives (MTBE, ETBE, TAME and DIPE), have been measured.

In order to provide correlative methods to be used in computer-aided design, data were directly correlated with polynomial functions. Density and vapour pressures were simultaneously correlated by a lattice equation of state. Ultrasonic velocities were compared through isentropic compressibility description with FLT. Satisfactory results were obtained with all predictive and correlative models.

Acknowledgements

This study was supported by the CTQ2004-03346/PPQ Project (Ministerio de Educación y Ciencia, Secretaria General de Política Científica y Tecnológica, España).

Miguel Iglesias and Rafael Gonzalez-Olmos wish to thank the Chemical Engineering Post-Graduation Program of Federal University of Bahia for their support in the development of his research.

The authors would like to thank REPSOL-YPF for provide ETBE for this study.

References

- [1] R.A. Deeb, K. Chu, T. Shih, S. Linder, I. Suffet, M.C. Kavanaugh, L. Alvarez-Cohen.. *Environ. Eng. Sci.*, **20**, 433 (2003).
- [2] H.P.H. Arp, T.C. Schmidt.. *Environ. Sci. Technol.*, **38**, 5405 (2004).
- [3] M.A. Krahenbuhl, J. Gmehling.. *J. Chem. Eng. Data*, **39**, 759 (1994).
- [4] R.K. Toghiani, H. Toghiani, G. Venkateswarlu.. *Fluid Phase Equilib.*, **122**, 157 (1996).
- [5] A. Arce, J. Martínez-Ageitos, E. Rodil, A. Soto.. *Fluid Phase Equilib.*, **165**, 121 (1999).
- [6] S. Loras, A. Aucejo, R. Muñoz.. *Fluid Phase Equilib.*, **194**, 957 (2002).
- [7] S. Gupta, J.D. Olson.. *Ind. Eng. Chem. Res.*, **42**, 6359 (2003).
- [8] M. Iglesias, S. Mattedi, R. Gonzalez-Olmos, J.M. Goenaga, J.M. Resa.. *Chemosphere*, **67**, 384 (2007).
- [9] Gonzalez-Olmos, R.; Iglesias, M. *J. Chem. Journal of Chemical Thermodynamics*, (2008) (in Press).
- [10] S. Mattedi, F.W. Tavares, M. Castier.. *Fluid Phase Equilib.*, **142**, 33 (1998).
- [11] B. Jacobson.. *Acta Chem. Scand.*, **6**, 1485 (1952).
- [12] D.C. Lamdaverde-Cortes, A. Estrada-Baltazar, G.A. Iglesias-Silva, K.R. Hall.. *J. Chem. Eng. Data*, **52**, 1226 (2007).
- [13] A. Jangkamolkulchai, G.C. Allred, W.R. Parrish.. *J. Chem. Eng. Data*, **36**, 481 (1991).
- [14] A. Rodríguez, A. Canosa, J. Tojo.. *J. Chem. Thermodyn.*, **31**(8), 1009 (1999).
- [15] E. Mascato, L. Mosteiro, M.M. Pineiro, B.E. de Cominges, M.M. Mato, J.L. Legido.. *J. Therm. Anal. Calorim.*, **70**, 235 (2002).
- [16] K.V.N.S. Reddy, P.S. Rao, A. Kirshnaiah.. *J. Mol. Liq.*, **135**, 14 (2007).
- [17] C.M. Kinart, A. Cwikinska, W.J. Kinart.. *J. Therm. Anal. Calorim.*, **84**, 535 (2006).
- [18] A. Arce, E. Rodil, A. Soto. *J. Chem. Eng. Data*, **42**, 721 (1997).
- [19] J. Linek. *Collect. Czech. Chem. Commun.*, **52**, 2839 (1987).
- [20] J.D. Ye, C. Tu.. *J. Chem. Eng. Data*, **50**(3), 1060 (2005).
- [21] H.W. Chen, C.H. Tu.. *J. Chem. Eng. Data*, **51**, 261 (2006).
- [22] U. Domanska, J. Lachwa, T.M. Letcher.. *J. Chem. Thermodyn.*, **34**, 885 (2004).
- [23] K.V.N.S. Reddy, G.S. Reddy, A. Krishnaia.. *Thermochim. Acta*, **440**(1), 43 (2006).
- [24] P. Bevington.. *Data Reduction and Error Analysis for the Physical Sciences*, McGraw-Hill, New York (1969).
- [25] J.O. Valderrama.. *Ind. Eng. Chem. Res.*, **42**(8), 1603 (2003).
- [26] W.H. Press, B.P. Fannery, S.A. Teutolsky, W.T. Vetterling. *Numerical Recipes. The Art of Scientific Computing (Fortran Version)*, Cambridge University Press, New York (1989).
- [27] T.E. Daubert, R.P. Danner. *Physical and Thermodynamic Properties of Pure Compounds, Data Compilation*, Taylor and Francis, New York (1985).
- [28] C. Tsonopoulos, J.H. Dymond. *Fluid Phase Equilib.*, **133**, 11 (1997).